Analysis of Drone-based Last-mile Delivery Systems under Aerial Congestion: A Continuum Approximation Approach

Ruifeng She
Yanfeng Ouyang

CENTER FOR CONNECTED AND AUTOMATED TRANSPORTATION

ILLINOIS CENTER FOR TRANSPORTATION

DISCLAIMER

Suggested APA Format Citation:

She, R., & Ouyang, Y. (2023). *Analysis of drone-based last-mile delivery systems under aerial congestion: A continuum approximation approach* (Report No. ICT-23-014). Illinois Center for Transportation. https://doi.org/10.36501/0197-9191/23-014

Contacts

For more information:

Yanfeng Ouyang
University of Illinois Urbana-Champaign
2129E Newmark Civil Engineering Bldg
yfouyang@illinois.edu
https://ict.illinois.edu

CCAT
University of Michigan Transportation Research Institute
2901 Baxter Road
Ann Arbor, MI 48152
uumtri-ccat@umich.edu
(734) 763-2498
www.ccat.umtri.umich.edu

TECHNICAL REPORT DOCUMENTATION PAGE

1. Report No. ICT-23-014	2. Government Accession No. N/A	3. Recipient's Catalog No. N/A		
4. Title and Subtitle Analysis of Drone-based Last-mile Delivery Systems under Aerial Congestion: A Continuum Approximation Approach		5. Report Date August 2023		
		6. Performing Organization Code N/A		
7. Authors Ruifeng She (https://orcid.org/0000-0002-1617-9821) and Yanfeng Ouyang (https://orcid.org/0000-0002-5944-2044)		8. Performing Organization Report No. ICT-23-014 UILU-ENG-2023-2014		
9. Performing Organization Name and Address Illinois Center for Transportation Department of Civil and Environmental Engineering University of Illinois at Urbana–Champaign 205 North Mathews Avenue, MC-250 Urbana, IL 61801		10. Work Unit No. N/A		
		11. Contract or Grant No. Grant No. 69A3551747105		
12. Sponsoring Agency Name and Address Center for Connected and Automated Transportation University of Michigan Transportation Research Institute 2901 Baxter Road Ann Arbor, MI 48152		13. Type of Report and Period Covered Final Report		
		14. Sponsoring Agency Code		

16. Abstract

This paper presents a systematic analysis and design framework for a spectrum of last-mile delivery systems that leverage unmanned aerial vehicles (UAVs). Four distinct modes are considered: (1) direct drone deliveries from a fixed depot; (2) drone deliveries from parked trucks that carry bulk parcels to customer neighborhoods; (3) drone deliveries from nonstopping trucks that tour customer neighborhoods; and (4) as a benchmark, traditional truck-based home deliveries. We present a new continuum-approximation approach that is used for analysis of both truck routing and aerial-UAV traffic. We compared the operational cost and efficiency of different delivery schemes to reveal how a certain scheme is the most efficient under various scenarios. We demonstrate the applicability of our model on expansive real-world roadway networks and further conduct analysis on grid networks, yielding key analytical insights. The drone-based delivery is demonstrated to be superior to conventional truck-only delivery, suggesting a significant potential for socioeconomic benefit. It is observed that when servicing a relatively low demand over a small area, dispatching drones directly from the distribution facility is the most efficient method. As the demand grows or spans a wider area, collaborative strategies are preferred, as they better cope with certain aspects, such as the long line-haul cost or the ramping aerial congestion, by striking a balance between efficiency and flexibility.

17. Key Words Unmanned Aerial Vehicle, UAV, Drone, Vehicle Routing, Congestion, Traffic Equilibrium	18. Distribution Statement No restrictions. This document is available through the National Technical Information Service, Springfield, VA 22161.		
19. Security Classif. (of this report) Unclassified	20. Security Classif. (of this page) Unclassified	21. No. of Pages 31	22. Price N/A

Form DOT F 1700.7 (8-72)   **Reproduction of completed page authorized**

ACKNOWLEDGMENT, DISCLAIMER, MANUFACTURERS' NAMES

EXECUTIVE SUMMARY

The emergence of autonomous and connected trucks (ACTs) brought about significant changes in freight delivery, impacting efficiency, safety, energy consumption, and infrastructure durability. One important change has been the formation of truck platoons, made feasible and practical by the intelligent technologies integrated into ACTs. Although truck platooning has benefits in fuel consumption and traffic efficiency, it requires substantial computational resources to optimize the aerodynamic performance of the platoon. To overcome these challenges, data-driven surrogate models have been developed that significantly improve computational efficiency. We compared the performance of the generalized additive model and neural network surrogate model to baseline data-driven models that included linear regression and support-vector regression. The results demonstrate the effectiveness of using surrogate models for drag-force prediction and highlight their potential for real-time applications in truck platooning.

Furthermore, a fuel-consumption and cost analysis of truck freight delivery was conducted as case study. The real wind-speed and -direction data were collected from a wind station close to the corridor. The length of the corridor was 161 km (100 mi), with high platoonability. The wind history along the highway segment was analyzed, and delivery windows were established based on the fluctuations in wind speed and direction. The study demonstrated the potential for truck platooning to reduce fuel consumption. Additionally, by automating truck delivery, the fuel consumption for truck operation and the required number of truck drivers were reduced, which made the bulk of the operational cost less than in the conventional delivery scheme.

TABLE OF CONTENTS

LIST OF FIGURES

CHAPTER 1: INTRODUCTION

OVERVIEW

Unmanned aerial vehicles (UAVs), more commonly known as drones, are rapidly gaining recognition within the logistics industry as viable alternatives for fulfilling short-range mobility needs, as they have demonstrated superior efficacy due to their ability to traverse low-altitude airspace, facilitating faster, more automated, and more direct point-to-point deliveries (Jokisch and Fischer, 2019). Leading logistics enterprises are capitalizing on these advantages by considering drones for last-mile delivery services. In 2016, Amazon's Prime Air successfully completed the first commercial drone delivery, transporting a package of 2.6 kg (5.73 lbs) over 7 mi in just 13 min (Perlow, 2016). Since then, FedEx, UPS, and DHL have all launched dedicated initiatives to explore this technology's potential (Frachtenberg, 2019), signaling a trend that's gradually gaining public trust. This momentum is also being met with regulatory adaptation. In 2020, the US Federal Aviation Administration (FAA) granted Amazon approval to deploy drone fleets for parcel delivery within the United States, albeit under stringent safety regulations (Palmer, 2020). Similarly, various government agencies are proactively developing policies to facilitate the large-scale industrial deployment of drone-based deliveries (Zoldi, 2021), demonstrating their increasing recognition as a practical and beneficial logistic solution.

Innovations and adaptations to accommodate drone-based delivery have also been reflected in the research sphere, with numerous studies developing conceptual designs for these systems. For instance, the "drone's nest" concept posits facilities that function as both warehouses and centralized dispatching centers, akin to distribution centers in traditional last-mile logistics. In these scenarios, each drone is directly dispatched from the facilities, making a round trip to carry the parcel to the assigned customer. In this paper, we refer to this family of operations as depot–drone (DD). Shavarani et al. (2019) advanced this idea by formulating a facility–location problem, optimizing charging- and launching- station placement to minimize costs and avoid overly long trips. Similarly, Chauhan et al. (2022) studied a facility–location and online-demand-allocation problem in delivery services using drones. Other bodies of research have concentrated on optimizing drone-delivery routes, with some considering elements such as varying drone capacities, priority of deliveries, and dynamic demand (Chiang et al., 2019; Kim, 2017). Dorling et al. (2016) put forth a vehicle-routing problem designed to minimize total operating costs for sequential drone deliveries. Pachayappan and Sudhakar (2021) proposed a mathematical model and heuristic solution for planning optimal pickup and delivery routes in drone operations.

Existing drone models are typically capable of carrying one parcel at a time, therefore fulfilling one delivery demand per trip. This arrangement necessitates operating a large fleet of drones concurrently, which can result in aerial traffic congestion, particularly around active neighborhoods or concentrated-demand areas. Although research on the impact of such congestion is still limited, it's an area that warrants attention. Evaluating drone traffic presents a unique challenge. Traditional congestion models, such as the family of min-cost flow problems with nonlinear link cost, struggle to represent the myriad route options in a reasonable graph of the airspace. In response, She and Ouyang (2021) took a continuous approach, defining the steady-state traffic equilibrium as a system

of partial differential equations (PDEs). They illustrated how local traffic delays for drones can diminish operational efficiency and increase battery-power consumption. This research also pointed out that although drones extend service reach over long distances, high-demand areas may limit the effective service range. In addressing this dilemma, a hybrid delivery system that combines drones with traditional surface-transportation vehicles (for line-haul shipments) presents itself as a promising solution. The conceptual framework for this hybrid system involves a truck carrying a large number of parcels and a fleet of drones, traversing the city along a designated route. Drones then, deployed from the truck, deliver parcels to customers' doorsteps. In this simplest form of collaboration, which we refer to as stationary truck–drone (STD), drones can be dispatched when the truck stops at certain nodes, mimicking the method discussed by She and Ouyang (2021). Such a collaboration could be made even more efficient by integrating drones with moving delivery vehicles, which we refer to as mobile truck–drone (MTD), leveraging the strengths of each vehicle type. Carlsson and Song (2018) proposed allowing drones to be dispatched from a moving truck and then catch up with the truck later. This approach not only extends the drone's service range but also enhances the accessibility of the truck and reduces its route length, optimally balancing efficiency and flexibility. Liang and Lui (2022) recently conducted a comprehensive review of such efforts. The synchronized routing of trucks and drones has been termed the truck–drone routing problem (TDRP) (Laporte, 2009). Its simplified version, which involves only one truck and one drone, is known as the traveling-salesman problem with drones (TSPD) or the flying-sidekick, traveling-salesman problem (FSTSP), formulated as a mixed-integer program by Murray and Chu (2015). Although the TDRP (Laporte, 2009) and TSPD (Murray and Chu, 2015) models offer valuable insight into efficient vehicle routing, they do not fully capture the complexity of real-world logistics scenarios, which often involve more than two vehicles (trucks and drones). In response, some studies have focused on the coordination of a single truck with a fleet of drones (Murray and Raj, 2020; Carlsson and Song, 2018). This problem also aligns closely with the school bus–routing problem (SBRP) (Park and Kim, 2010), which simultaneously involves selecting bus stops and routing the bus. The solution to the SBRP primarily follows a location-allocation-routing strategy, sequentially selecting bus stops, assigning demand to bus stops, and designing bus routes. Meanwhile, considering demands as continuously emerging in a region transforms the problem into one of covering the region with an optimally placed swath (i.e., the service range of the drones from the truck), also referred to as the covering-path problem. This problem has been explored in various forms in the literature (Zeng et al., 2019) and is usually solved via a decomposition-routing strategy.

In a closer look at congestion issues, She and Ouyang (2022) employed the steady-state, traffic-equilibrium model to evaluate delivery efficiency under various operational conditions in an area served by a single moving truck. They noted the need for collaborative routing among multiple trucks to service a large domain, taking into account the finite truck capacity. Going further, to consider a fleet of trucks each equipped with multiple drones, Wang and Sheu (2019) introduced the vehicle-routing problem with drones (VRPD). This model features trucks hauling parcels and drones among a set of stationary, ground-based hubs. However, joint optimization for the discrete routing decisions of trucks and drones is undoubtedly challenging; and so far, only worst-case scenarios have been studied. With this in mind, a possible approach is to combine the continuous-traffic-equilibrium model for drone routing in hybrid delivery with the family of discrete VRP models for truck routing, naturally following a partition-first, route-second philosophy. Here, the large delivery domain is first

decomposed into regions, each served by a single truck. The routes of a fleet of trucks are then collectively determined to minimize overall operational costs, while ensuring all demands in all areas are serviced.

OBJECTIVES

Although various drone/truck–drone delivery schemes have been proposed, each has distinct advantages that may make it suitable for various scenarios. To best meet the varying needs of different demand characteristics over the space, it may be beneficial to consider a range of delivery schemes to be simultaneously deployed. Each of the schemes potentially requires specific infrastructure or technological investment, such launching devices on trucks to enable drone launching/landing in motion. However, as of this writing, there is no known research that addresses collaborative routing decisions for a hybrid delivery system that explicitly takes into consideration a variety of delivery schemes, vehicle types, and aerial-traffic congestion.

This paper seeks to fill that gap by making several contributions. First, the paper proposes a practical design framework to determine decisions for drone and truck routing in a collaborative last-mile delivery system. This system considers multiple potential delivery modes for local deliveries. Meanwhile, multiple types of trucks can be operated, each truck compatible with a certain set of delivery modes. By following a partition-first, route-second philosophy, the delivery domain is first decomposed into disjoint regions. Each of these regions has approximately homogeneous demand characteristics and is to be serviced with one mode, by one truck, in one visit. The optimal strategy for servicing each region is determined in conjunction with the routing strategies of the trucks. The collective routing decisions over regions are modeled in a variant of the multi-type, multimode vehicle-routing problem as a mixed-integer program, and an efficient heuristic algorithm is proposed.

Second, we consider multiple candidate delivery schemes that facilitate drones and trucks for delivery in different manners (i.e., DD, STD, and MTD). These schemes are conceptually illustrated in Figure 1, in which the delivery region is a circle over a roadway network formed by square grids, and a depot located at the southwest corner conducts the delivery. The delivery costs and efficiency of serving a region with each candidate mode are examined and compared, providing the basis for determining the optimal routing of trucks in the integrated design framework. Last, the applicability of the proposed design framework is demonstrated on both a grid network and real-world networks. A sensitivity analysis is also conducted with respect to key parameters, to draw operational insights.
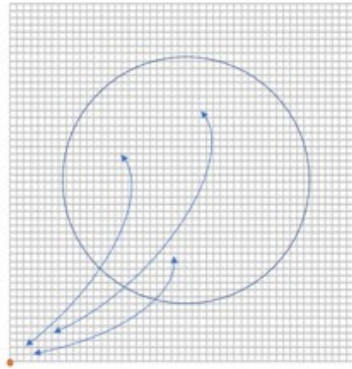
(a) Depot–drone
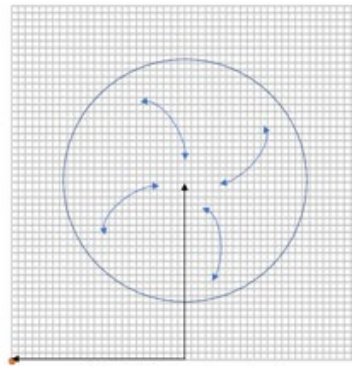
(b) Stationary truck–drone
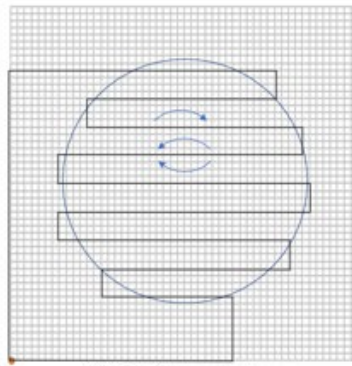
(c) Mobile truck–drone
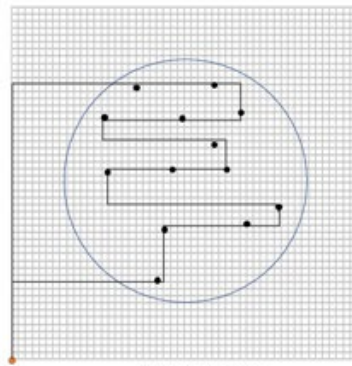
(d) Truck only

Figure 1**. Diagrams. Four modes of delivery schemes.**

CHAPTER 2: CONTINUOUS MODELS FOR TRUCK–DRONE DELIVERY SYSTEMS

In this section, we succinctly introduce a few model components that are associated with two drone delivery strategies: one from a stationary point and one from a moving truck.

These elements will subsequently form the building blocks of the design framework in this paper.

DRONE DELIVERY FROM A STATIONARY POINT

Consider a continuous, closed domain Ω where the logistics carrier operates a large fleet of drones from a central depot to serve the demand within the domain. These demands are assumed to randomly emerge at a time-invariant yet spatially dependent inflow rate, $\rho_0(x), \forall\, x \in\, \Omega$. The local traffic condition in the low-altitude airspace at steady state is indicated by a continuous density function. In the absence of traffic congestion, drones can travel freely at their peak speed, $v_{d,0}$. The impact of traffic congestion is encapsulated by the degradation of drone speed, estimated as a nonincreasing function of the local traffic density (She and Ouyang, 2022). Some earlier work described travel speed as a function of the local flux instead; e.g., as by She and Ouyang (2021).

Drones are presumed to communicate and exchange information; however, each independently seeks its optimal route to minimize its individual total travel cost. If all drones adhere to such routes, with no drone able to reduce its own travel cost through a unilateral path modification, the system is said to have reached the user equilibrium per Wardrop's principle (Wardrop, 1952). To find these optimal routes, we introduce a continuous potential function that equals the total travel cost for a drone to travel from x to its destination along the least-cost route. As demonstrated by She and Ouyang (2021), the equilibrium condition can be represented as a system of PDEs that can be solved using a specialized finite-element algorithm.

The resulting potential function from the PDE solution provides information on each drone's travel cost under equilibrium conditions. Furthermore, the optimal route for each drone can be constructed from this solution using Euler's method. For modeling simplicity, we consider a domain of a certain regular shape (e.g., a circle) with a homogeneous demand rate ρ_0 across the domain. The key output is the average round-trip travel time, denoted as $\hat{\phi}_1(|\Omega|, \rho_0)$, We solve the PDEs over a range of likely combinations of ρ_0 and $|\Omega|$ and in so doing providing a surrogate model that can be used to interpolate $\hat{\phi}_1(|\Omega|, \rho_0)$ for a generalized domain. Such a model provides a basis to evaluate the performance of the delivery system proposed in later sections.

DRONE DELIVERY FROM A MOVING SOURCE

A hybrid delivery scheme involves a mobile launching platform, such as a truck, which transports drones and goods to an optimal distance from the customer locations. From there, drones embark on their delivery mission and subsequently return to the truck positioned further along the route. By strategically coordinating the drone and truck operations, it's possible to mitigate the adverse effects of traffic congestion, thereby striking a balance between flexibility and efficiency of both delivery

modes. Suppose that the delivery truck operates at a constant truck speed v_t. Meanwhile, drones are dispatched to make direct deliveries to customers on both sides of the road within a perpendicular distance of W from the truck. If the demand density in the domain is uniform, the drone traffic near the truck can be considered in a steady state. The study by She and Ouyang (2022) has demonstrated that the traffic-equilibrium condition, as perceived from the truck's viewpoint, can be formulated as a system of PDEs involving the potential function. A physics-informed, neural network (PINN) algorithm equipped with suitable convergence-enhancing techniques is then employed to solve the PDEs. A surrogate model yielding the average delivery time $\hat{\phi}_2(W, v_t, \rho_0)$ can again be constructed.

CHAPTER 3: HYBRID DELIVERY-SYSTEM DESIGN

Consider service domain Ω, in which delivery demands uniformly emerge at rate $\bar{\rho}_0$. The logistics carrier operates a fleet of drones and trucks and conducts service every H units of time within a duration window of H'. As such, the demand upon delivery is regulated as $\rho_0 = \left(\frac{H}{H'}\right)\bar{\rho}_0$. Each truck belongs to one of the predefined truck types $l \in L$, which can be used to conduct certain delivery modes $m \in M$. Different types of trucks are likely to have distinct characteristics, such as trucking costs, denoted as $\{w_t^l, \forall\, l \in L\}$ per unit distance, and cargo capacities, denoted as $\{Q^l, \forall\, l \in L\}$. All types of trucks are assumed to always operate at a constant speed v_t except for conducting the MDT delivery mode, for which we specify the designed truck speed for serving region c as $v_{t,c}$.

In designing most logistics systems, at least two phases of decisions must be made sequentially. The tactical phase concerns long-term decisions, such as the fleet size of vehicles—both trucks and drones—to invest in and maintain; and the frequency of delivery, often advertised as a service standard to the customers. These decisions are made before the service is provided, hence are based on a belief in the expected demand pattern over the service domain. Specifically, suppose we possess, from analyzing historical data, the steady-state, demand-rate function $\bar{\rho}_0(x)$ that describes the expected arrival rate of demand. We wish to determine the number of drones and trucks of all types that is required to sustain a service that makes a delivery at a designed headway H. The operational phase, in contrast, concerns mission-specific decisions. Upon every delivery mission, the logistics carrier observes a set of discrete demand points D and determines the routing of trucks and drones to best serve all demands using the available fleets. In both phases, the complete delivery plan must be made; and the design components largely overlap, except for the treatment of the demand (i.e., as a continuous function or as a set of discrete points). In this section, we focus on the tactical phase and propose the integrated framework, which (taking the continuous demand distribution over the domain as input) aims to determine optimally all pertinent strategies and decisions to carry out the delivery service. The design workflow is decomposed into solving several subproblems; for each of which, we state the key objective, input, and output, and suggest an efficient method to yield a near-optimal solution. Adaptations are introduced along the way as needed to cope with discrete demand for the operational phase.

DELIVERY-DOMAIN PARTITIONING

Considering the continuous demand-rate-distribution function $\bar{\rho}_0(x)$, we partition the service domain Ω into nonoverlapping subregions $\{\Omega_c, \forall c \in C\}$, such that the demand rate in each subregion is approximately homogeneous. That is, we wish to minimize the nonhomogeneity in each subregion c, which can be measured by a continuous variance-like metric:

$$\frac{1}{|\Omega_c|} \int_{\Omega_c} (\bar{\rho}_0(\mathbf{x}) - \bar{\rho}_{0,c})^2 d\mathbf{x}$$

Figure 2. Equation. Density non-homogeneity metric.

where $\bar{\rho}_{0,c}$ denotes the average demand rate in Ω_c. Additionally, it is convenient to require each subregion to be convex, such that the covering swaths introduced in Chapter 3 can be constructed with simple approaches without incurring excessive deadheading. Last, the demand within each subregion should be served by a single visit of a truck of any type without exceeding its capacity.

A simple yet efficient approach to identifying density-homogeneous partitions is to construct the level contour of $\bar{\rho}_0(x)$. As such, the difference in demand rate in each contour level is bounded by the contour interval. The resultant contour levels are nonoverlapping polygons but are very likely nonconvex. There exist abundant methods to further decompose arbitrary shapes into convex polygons; but for well-shaped contour levels resulting from choosing a reasonable contour interval, a trapezoidal decomposition method (Choset, 2000) would be sufficient. To ensure the capacity requirements hold, the subregions are further refined into $\left\lceil \frac{|\Omega_c| H \bar{\rho}_{0,c}}{min_l Q^l} \right\rceil$ parts as needed with approximately the same areas. For two-dimensional geometries, we find the centroidal Voronoi tessellations generated by the Lloyd algorithm (Du et al., 2006), using low-variance seeds generated by the quasi-random Halton sequence (Wang and Hickernell, 2000), yields satisfying refinement.

Denote $G = (V, E)$ as the directed roadway network in the domain. We can identify the boundary nodes for this subregion as $B_c = \{i \in V : x(i) \in \Omega_c, x(j) \notin \Omega_c, \forall (i,j) \in E\}$, where $x(i)$ denotes the spatial coordinate of node i. Alternatively, the boundary node can be defined as the intersection of the edges with the boundary of Ω_c. Such an approach can be a more accurate graph reduction of the subregions but requires additional treatment to recover the original graph connectivity. The interior nodes of Ω_c are identified as $I_c = \{i \in V \setminus B_c : x(i) \in \Omega_c\}$. The subgraph spanned by B_c, I_c, and E forms the basis for the problems discussed in later subsections.

Now suppose we wish to perform domain decomposition based on the discrete demand D observed in the operational phase. First, we divide D into a set of nonoverlapping exhaustive clusters $\{D_c, \forall c\}$, such that the demand density in each cluster is approximately homogeneous, while the difference in demand density is large across clusters. After the demand points are clustered, the convex hull of cluster c naturally gives a polygonal representation of subregion Ω_c. The combinatorial formulation of the clustering problem is well known to be NP-hard and intractable to be solved exactly. However, there exists plenty of heuristics to yield suboptimal solutions, such as the hybrid density-based clustering algorithm (HDCA)(Fahim, 2018), which is an extension to the well-known DBSCAN algorithm (Schubert et al., 2017). In summary, the algorithm identifies clusters by iteratively expanding points within a cutoff distance from a member point. Upon constructing a new cluster, an initial point of d_0 is selected; and the cutoff distance is often set as the average distance from d_0 to its q_1 nearest points. A candidate point is clustered only if it has at least q_2 neighbors within the cutoff distance. As such, the average density in the cluster is gauged by the neighborhood of the initial point and is maintained as the cluster expands. We hence have control over the clustering behavior through the two parameters, q_1 and q_2. Here, q_1 influences the shape skewness of the clusters. For example, letting $q_1 = 1$ allows a chain of points to be identified as a cluster. It was shown by experiments that by using reasonable q_1 values (e.g., larger than 4), the algorithm yields geometrically convex clusters. Further, if q_1 and q_2 are close in value, the algorithm yields a large

number of fine clusters with high homogeneity, and vice versa. In addition, the capacity constraints can be easily enforced by adding $min_{l \in L} Q^l$ as a terminating threshold in the expanding steps.

DELIVERY-REGION-COVERING COST

A single region can be served by one of the four delivery modes presented in Figure1, i.e., DD, STD, MTD, or truck-only, coded by $m \in M = \{0, 1, 2, 3\}$, respectively. Denote $\widetilde{w}_{ij}^{m,l}$ as the covering cost and $T_{ij}^{m,l}$ as the service time, respectively, when a type-l truck serves region c with mode m; and the truck enters and exits region c via node $i, j \in B_c$. We evaluate $\widetilde{w}_{ij}^{m,l}$ for all possible combinations of i, j, l, and m, which will later be used as inputs at the upper level, such that the optimal choice of access nodes, together with pertinent operational decisions, will be determined in conjunction with the routing of the truck that serves this region.

Depot–Drone (DD)

We first consider the depot–drone strategy. Suppose drones are directly dispatched from a depot located S units of distance away from the center of the region. The optimal paths of drones depend on S and the characteristics of Ω_c and hence would require solving the PDEs with boundary conditions specifically modified for each region. However, a feasible solution can be approximated to avoid expensive and repetitive computations. First, we approximately treat the convex as a circle. According to the numerical results by She and Ouyang (2021), aerial congestion mainly takes effect around the depot near the ground; and drones can travel almost at a free-flow speed at their peak heights. With such an insight, we construct a feasible drone-routing scheme, as presented in Figure 2. Consider the inbound (return) leg, where the trajectory of each drone is split into the ascending branch and descending branch at its peak height from the ground. Drones first identify the optimal paths as if the depot is located at the center of the delivery region. Each drone follows the ascending branch of its individual optimal path toward the peak height, travels horizontally to the same relative position from the depot, and then descends and lands at the depot along the descending branch of the optimal path.
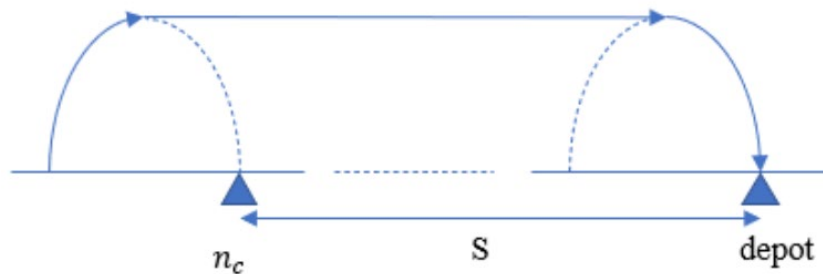
Figure 3. Diagram. A feasible scheme of drone-only delivery.

As such, the complete delivery route for a drone equivalently consists of the local parts along the optimal path and the line-haul part of length S involving only horizontal movement. The round-trip delivery time for an average drone using this feasible trajectory is given by $\hat{\phi}_1(|\Omega_c|, \rho_{0,c}) + 2S/v_{d,0}$.

Using Little's formula, the number of drones required to sustain the service in the region can be estimated as

$$\rho_0 |\Omega_c| \left(\hat{\phi}_1(|\Omega_c|, \rho_{0,c}) + \frac{2S}{v_{d,0}} \right).$$

Figure 4. Equation. Number of drones required.

Additionally, from the customers' perspective, the service frequency impacts the customers' waiting time and the value depreciation of the goods. Assuming nondiscriminative service (i.e., parcels are delivered in random orders without prioritizing certain customers), the average waiting time of each customer is half of the headway H.

The average delivery cost per parcel is computed as

$$\tilde{w}_{ij}^{0,l} = \left(w_d + \frac{w_{df}}{H'} \right) \left(\hat{\phi}_1(|\Omega_c|, \rho_{0,c}) + \frac{2S}{v_{d,0}} \right) + \frac{w_c H}{2}, \forall i, j \in \mathcal{B}_c, \forall l \in \mathcal{L}.$$

Figure 5. Equation. Average delivery cost for drone-only delivery.

where w_d denotes the drones' battery-power-consumption rate, w_{df} denotes the drones' preparation cost per drone per delivery window, and w_c denotes the average cost per unit time incurred by the customers, respectively. Here, $T_{ij}^0 = H' \leq H$, where $H' = H$ means the drone-delivery service is conducted continuously (e.g., 24 hours a day)

Stationary Truck–Drone (STD)

When serving region c with STD mode, the truck temporarily stops at a street node closest to the center of the domain c, denoted as n_c. The drones are dispatched from the stopped truck to conduct delivery service within the region, and the drones' operation and preparation costs are evaluated in the same way as the local parts in Eq.(3).

The overall operating cost is given by

$$\tilde{w}_{ij}^{1,l} = \left(w_d + \frac{w_{df}}{H'} \right) \hat{\phi}_1(|\Omega_c|, \rho_{0,c}) + \frac{w_c H}{2} +$$
$$\left(w_t^l + \frac{w_{man}}{v_t} \right) (P(i, n_c) + P(n_c, j)), \forall i, j \in \mathcal{B}_c, \forall l,$$

Figure 6. Equation. Average delivery cost for STD delivery.

where $P(i,j)$ denotes the shortest path distance from node i to node j via edges in E. Meanwhile, the required drone fleet size is estimated as $\rho_0|\Omega_c|\,\hat{\phi}_1(|\Omega_c|,\rho_{0,c})$; and the service time for the region is given by

$$T_{ij}^1 = H' + \frac{P(i,n_c) + P(n_c,j)}{v_t}, \forall i,j \in \mathcal{B}_c.$$

Figure 7. Equation. Service time for STD delivery.

Mobile Truck–Drone (MTD)

With drones capable of simultaneously fulfilling local deliveries, the truck traverses the delivery region along a path such that all demands are served. We assume that the carrier employs the swath algorithm for the probabilistic traveling-salesman problem as detailed by Daganzo (1984) to cover the region c. According to this algorithm, the truck traverses the region along the center of a "swath" with a width of $2W_c$ (where W_c equivalently represents the span of the service range on each side of the swath), while maintaining a constant speed $v_{t,c}$. The optimal design of the service strategy thus poses a nontrivial covering-path problem depending on Ω_c and $\bar{\rho}_0$. We approach this problem by first choosing W_c and $v_{t,c}$ that optimize the asymptotic performance of the delivery operation and subsequently constructing the swath.

Suppose that the delivery region is covered by a dense roadway network that enables trucks to travel in any direction for any distance. Such a network allows a swath of length $|\Omega_c|/2W_c$ to perfectly cover the region. Meanwhile, a fleet of $2W_c v_{t,c}\bar{\rho}_0 H\hat{\phi}_2$ drones must be simultaneously operated to sustain the delivery service. The average delivery cost is given by

$$\tilde{w}_{ij}^{2,l} = w_d\hat{\phi}_2 + \frac{2w_{df}W_c v_{t,c}\hat{\phi}_2}{|\Omega_c|} + \frac{w_{man}/v_t + w_t^l}{2W_c\bar{\rho}_0 H}, \forall i,j \in \mathcal{B}_c, \forall l \in \mathcal{L},$$

Figure 8. Equation. Average delivery cost for MTD delivery.

and in so doing, we determine W_c and $v_{t,c}$ such that the average delivery cost is minimized for Ω_c.

An efficient heuristic to construct such a feasible swath ending with designated entry and exit points i and j can be achieved in two steps. The first step is to identify a subset of nodes in $I_c' \subseteq I_c$ that are roughly $2W_c$ apart, which represents a discrete aggregation of the demands, such that by visiting these nodes, all demands in Ω_c are considered serviced. We can find I_c' by masking I_c with a square mesh of size $2W_c$ and then include an interior node in I_c' if it is the closest node to the center of any of the squares. The second step is to visit all nodes in I_c' at least once in the most efficient way. This problem is essentially a traveling-salesman problem (TSP) with a given origin and destination pair (i,j), also referred to as the open-TSP, which can be reduced to a TSP with the addition of a dummy edge.

The TSP has been studied extensively and is known to be NP-complete. Although there exists plenty of solution algorithms (e.g., Lin-Kernighan (Helsgaun, 2000)), the superpolynomial running time can be of concern, considering that the problem must be solved for a large number of instances before every delivery mission. An efficient alternative heuristic to construct a near-optimal solution to the TSP is by performing a forward–backward sweep. To find the open-TSP path for the graph presented in Figure 3a, we first map a square mesh with a size of $2W$. Starting from one corner (e.g., the top-left corner), we construct the shortest swath to reach another corner (e.g., the bottom-right corner), while all meshes are visited, as illustrated in Figure 3c. A change of sweeping direction is applied to avoid deadheading due to the "inconvenient" positioning of the starting and ending point, as illustrated by the last two rows of the mesh in Figure 3c. This adaptation can be achieved easily in constant running time because the swath logic can be determined given the dimension of the mesh grid (i.e., odd or even numbers of rows and columns) and the starting/ending corners (i.e., same side on row, column, or diagonal). The order by which the nodes in I'_c are visited along the sweeping swath directly gives a feasible solution to the open-TSP, as given in Figure 3d. Deadheadings are then appended as necessary to connect to the desired entry/exit points. Note that, as compared to the optimal solution in Figure 3b, the feasible solution in Figure 3d is suboptimal, mainly due to the irregularity of the graph that does not align with the swath obtained from a grid. In reality, the assumption of a dense street network is very likely violated and will cause deteriorated performance. To compensate for such a deficit, we examine another swath by starting in a different direction, as presented in Figure 3e, and obtained a potentially improved solution in Figure 3f. The overall complexity to solve the open-TSP is linear to I'_c. Because various entry/exit points are to be evaluated for the region, we examine $4 \times 2 \times 3 = 24$ possible paths, starting with each of the four corners, along two possible directions, and ending at each of the other corners.

Denoting the optimal TSP length from i to j obtained using this approach as P^2_{ij}, we substitute it back into Eq.(6) to replace the swath length and recompute the average delivery cost as

$$\tilde{w}^{2,l}_{ij} = w_d \hat{\phi}_2 + \frac{2w_{df} W_c v_{t,c} \hat{\phi}_2}{|\Omega_c|} + \left(w_{man}/v_{t,c} + w^l_t \right) \frac{P^2_{ij}}{\bar{\rho}_0 H |\Omega_c|}, \forall i,j \in \mathcal{B}_c, \forall l \in \mathcal{L},$$

Figure 9. Equation. Average delivery cost for MTD delivery.

while the service time is given by $T^2_{ij} = \frac{P^2_{ij}}{v_{t,c}}$.
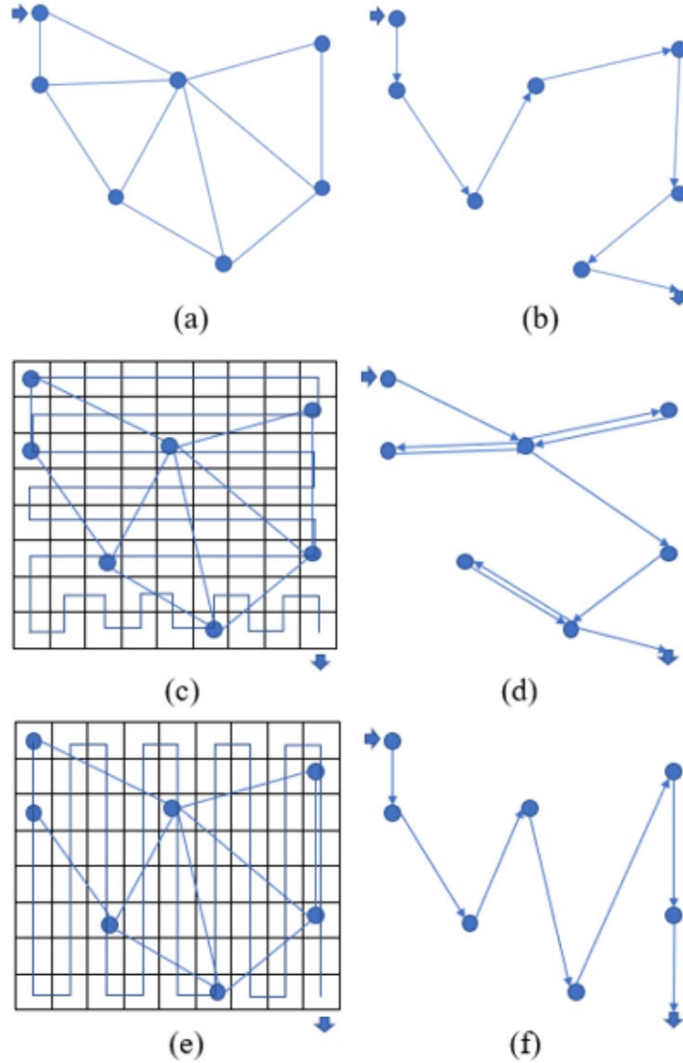
Figure 10. Diagrams. Covering path constructed by a forward–backward heuristics.

Truck-only Delivery

In certain urban areas, drone operation may be prohibited due to complex high-rising obstacles or regulatory restrictions, necessitating the inclusion of conventional truck-only delivery in a drone-based delivery system. The routing of trucks in the truck-only delivery mode is influenced by the locations of the specified demand points. Therefore, we specifically model and evaluate the truck-only delivery mode based on a set of discrete demand points D_c. During the tactical phase, the cost assessment can be obtained by averaging multiple instances of demands generated randomly from the desired distribution. We assume that the city permits temporary parking anywhere on its streets. For each delivery, the delivery personnel parks the truck at the nearest point on the street closest to the customer's location and walks to the customer's doorstep at a speed of v_{walk} over the distance h_d. Consequently, a subset of streets will be associated with specific demands and must be traversed by the truck. This task can be formulated as the rural-postman problem, which is a generalization of the Chinese-postman problem (Nobert and Picard, 1996). To specify the desired starting and ending

points i, j, we add a dummy edge (i, j) and connect i, j to all nodes in I_c Although the problem is NP-hard, heuristic algorithms exist to obtain near-optimal approximations, such as those based on balanced-graph construction and Tabu search (Corberán et al., 2000).

We denote the resulting path length as P_{ij}^3. The overall delivery cost per parcel can then be given as

$$\tilde{w}_{ij}^{3,l} = \left(w_t^l + \frac{w_{man}}{v_t} \right) \frac{P_{ij}^3}{\mathcal{D}_c} + \frac{w_{man}}{v_{walk}} 2 \sum_{d \in \mathcal{D}_c} h(d), \forall i, j \in \mathcal{B}_c, \forall l,$$

Figure 11. Equation. Average delivery cost for truck-only delivery.

and the service time is given by

$$T_{ij}^3 = \frac{1}{v_t} P_{ij}^3 + \frac{1}{v_{walk}} 2 \sum_{d \in \mathcal{D}_c} h(d), \forall i, j \in \mathcal{B}_c.$$

Figure 12. Equation. Service time for truck-only delivery.

TRUCK-ROUTE PLANNING

At the upper level, the logistics carrier determines the routing and scheduling strategy to serve all regions. The truck and drone fleet required to provide service in a reasonable working time incurs investment and maintenance costs, which must be accounted for. These decisions are intertwined; but a natural decision procedure consists of first generating routes that serve all regions, then accommodating these routes with a minimum number of vehicles.

The trucks are to be routed such that each region is accessed via a pair of boundary nodes and serviced by exactly one truck in a single visit. Conceptually, this problem is similar to the set-VRP, also known as the generalized VRP, where candidate nodes are separated into clusters; and exactly one node from each cluster is selected to be visited. The key difference is that our problem allows visiting 1 or 2 node(s) in each cluster, whereas the former corresponds to choosing the same node as both the entry and exit nodes. Further, the delivery cost for the region differs by the choice of access nodes, delivery modes, and truck types.

Let parameter $\mu_{ml} = 1$ if a truck of type l can be used to fulfill a delivery task of mode m. Each region can be served by one of the candidate modes using a truck of a compatible type. We call this problem a multi-type, multimodal, 2-set VRP (MM2VRP), which is defined as follows. To facilitate the previous development, we first construct an abstract graph, based on the roadway graph G, that is suitable for modeling and solving. When planning for the truck routes, we need to see only the boundary nodes B_c of subregion c and ignore all inner nodes in I_c. We create a dummy node for each region c at its center n_c, connect it to every boundary node of the region with edges $\{n_c\} \times B_c$, and assign zero weights. This dummy node will always be visited between the two access points. Further, we denote the interregional edges $\cup_{\forall c_2 \neq c_1} \{B_{c_1} \times B_{c_2}\}$, which connect the boundary nodes between

every pair of regions; and the depot-regional edges $\cup_{\forall\,c}\{\{o\}\times B_c\}$, which connect all boundary nodes to the depot node o. The abstract network to be considered herein is $G\_a = (V_a, E_a)$. Each edge is assigned a weight equal to the shortest path distance between the corresponding nodes in G.

The MM2VRP involves the following decision variables. Let binary variable $x_{ij}^k = 1, \forall\,(i,j) \in E_a, \forall\,k$ if route k traverses edge (i,j). Let binary variable $y_{cm} = 1, \forall\,c, \forall\,m \in M$ if region c is serviced with mode m. Let binary variable $z_{cl} = 1, \forall\,c, \forall\,l \in L$ if region c is serviced with a truck of type l. Let $u_{ij}, \forall\,(i,j) \in E_a$ denote the topological order by which the edges are traversed by any truck. To aid modeling, we also define the following auxiliary variables, which are determined by the decision variables. Let $\tau_{ij}^{ml} = 1, \forall\,i,j \in B_c, \forall\,c, m$ if nodes i and j are chosen to be the entry and exit points, respectively, to serve region c by a type-l conducting mode m. Let $\eta_{ij}^l = 1, \forall\,(i,j) \in E_a, \forall\,l$ if edge (i,j) is traversed by a truck of type-l. Let $\zeta_{ck} = 1, \forall\,c, k$ if region c is served by route k. Let $\sigma_{kl}, \forall\,k,l$ if route k is assigned to a truck of type l.

The solution to the MM2VRP must satisfy the following set of constraints. The flow conservation at intermediate nodes requires

$$\sum_{j\in\delta^-(i)} x_{ji}^k - \sum_{j\in\delta^+(i)} x_{ij}^k = 0, \forall k, \forall i \in V_a,$$

Figure 13. Equation. Flow-conservation constraints.

Where $\delta^-(i)$ and $\delta^+(i)$ denote the parents and children of node i, respectively.

We require each edge to be traversed in at most one route, as stated by

$$\sum_k x_{ji}^k \leq 1, \forall(i,j) \in \mathcal{E}_a.$$

Figure 14. Equation. Single-edge traverse constraints.

Note that these constraints apply to the abstract graph and allow multiple traversing of a real street edge as needed.

The number of active routes is given by

$$\sum_{j\in\delta^+(o)} x_{oj}^k \leq 1, \forall k.$$

Figure 15. Equation. Number of active routes.

The subtours are eliminated by

$$\sum_{j\in\delta^+(i)} u_{ij} - \sum_{j\in\delta^-(i)} u_{ji} = \sum_k \sum_{j\in\delta^-(i)} x_{ij}^k, \forall i \in \mathcal{V}_a \setminus \{o\},$$

$$u_{ij} \geq \sum_k x_{ij}^k, \forall(i,j) \in \mathcal{E}_a.$$

Figure 16. Equation. Subtour-elimination constraints.

Note that the topological order is defined over edges, as opposed to nodes as done in many conventional formulations (e.g., (Chirstofides et al., 1981). This purposeful choice allows visiting the same node twice in cases where the entry/exit nodes for a region are chosen to be the same.

Each dummy node, representing the fulfillment of the corresponding region, must be visited by exactly one route, given by

$$\sum_k \sum_{i\in\delta^-(n_c)} x_{in_c}^k = 1, \forall c,$$

Figure 17. Equation. Dummy-node constraints.

which, together with Eq.(13), enforces the entry-dummy-exit sequential visiting rule.

Meanwhile, each region must be serviced by exactly one mode and by one truck type, as stated by

$$\sum_m y_{cm} = 1, \forall c,$$

$$\sum_l z_{cl} = 1, \forall c,$$

$$y_{cm} = \sum_l z_{cl}\mu_{ml}, \forall c, m.$$

Figure 18. Equation. Region-visiting rules.

Each route must be assigned exactly one truck type, as given by

$$\sum_l \sigma_{kl} = 1, \forall k.$$

Figure 19. Equation. Truck type, route assignment.

The truck-capacity and route-duration constraints are respectively stated as

$$\sum_c \mathcal{D}_c \zeta_{ck} \le \sum_l Q^l \sigma_{kl}, \forall k,$$

$$\sum_c \zeta_{ck} \sum_{i,j \in \mathcal{B}_c} \tau_{ij}^{m,l} T_{ij}^m \le T_0, \forall k,$$

Figure 20. Equation. Truck-capacity and route-duration constraints.

where T_0 denotes the limit of route duration.

All auxiliary variables can be determined given $\{x_{ij}^k, \forall (i,j), k\}$, $\{y_{cm}, \forall c, m\}$, and $\{z_{cl}, \forall c, l\}$. These relations are stated as the following, as linear constraints.

For $\{\tau_{ij}^{ml}, \forall (i,j), m\}$:

$$\tau_{ij}^{m,l} \le \sum_k x_{n_c j}^k, \forall i, j \in \mathcal{B}_c, \forall c, \forall m, \forall l,$$

$$\tau_{ij}^{m,l} \le \sum_k x_{i n_c}^k, \forall i, j \in \mathcal{B}_c, \forall c, \forall m, \forall l,$$

$$\tau_{ij}^{m,l} \le y_{cm}, \forall i, j \in \mathcal{B}_c, \forall c, \forall m, \forall l,$$

$$\tau_{ij}^{m,l} \le z_{cl}, \forall i, j \in \mathcal{B}_c, \forall c, \forall m, \forall l,$$

$$\tau_{ij}^{m,l} \ge \sum_k x_{n_c j}^k + \sum_k x_{i n_c}^k + y_{cm} + z_{cl} - 3, \forall i, j \in \mathcal{B}_c, \forall c, \forall m, \forall l,$$

$$\tau_{ij}^{m,l} \ge 0, \forall i, j \in \mathcal{B}_c, \forall c, \forall m, \forall l.$$

Figure 21. Equation. Linear definition for tau.

For $\{\zeta_{ck}, \forall c, k\}$:

$$\zeta_{ck} = \sum_{i \in \delta^-(n_c)} x_{i n_c}^k, \forall c, k$$

Figure 22. Equation. Linear definition for zeta.

Denoting $C_k = \{c : \zeta_{ck} = 1\}$, and $M_k = \{m \in M : y_{cm} = 1, \forall c \in C_k\}$, $\{\sigma_{kl}, \forall k, l\}$ must satisfy

$$\sigma'_{kl} \leq \mu_{ml}, \forall m \in \mathcal{M}_k, \forall k, l,$$

$$\sigma'_{kl} \geq 1 + \sum_{m \in \mathcal{M}_k} (\mu_{ml} - 1), \forall k, l,$$

$$0 \leq \sigma_{kl} \leq \sigma'_{kl}, \forall k, l,$$

$$\sigma'_{kl} \geq 0, \forall k, l,$$

$$\sigma_{kl} = 0, \forall m \notin \mathcal{M}_k, \forall k, l.$$

Figure 23. Equation. Linear definition for sigma.

Here, σ'_{kl} is an additional auxiliary variable, which equals 1 if route k can be assigned to a truck of type l.

Denoting $K_l = \{k \in K : \sigma_{kl} = 1\}$ and $E_l = \{(i,j) \in E_a : x^k_{ij} = 1, \quad \forall k \in K_l\}$, $\{\eta^l_{ij}, \forall (i,j) \in E_a, \forall l\}$ must satisfy

$$\eta^l_{ij} = 1, \forall (i,j) \in \mathcal{E}_l, \forall l \in \mathcal{L},$$

$$\eta^l_{ij} = 0, \forall (i,j) \notin \mathcal{E}_l, \forall l \in \mathcal{L}.$$

Figure 24. Equation. Linear definition for eta.

Finally, the binary constraints on the explicit variables are given by

$$x^k_{ij} \in \{0,1\}, \forall (i,j) \in \mathcal{E}_a, \forall k,$$

$$y_{cm} \in \{0,1\}, \forall c, m,$$

$$z_{cl} \in \{0,1\}, \forall c, l,$$

Figure 25. Equation. Definition of decision variables.

while all auxiliary variables are implicitly enforced to be binary.

Denote the edge-traversing cost $\hat{w}^l_{ij} = w^l_t d_{ij}$ and the truck-dispatching cost per route $\bar{w}^l$ for type-l truck, respectively. The objective function minimizes the total operating cost, including the deadheading cost to travel between regions and depots, the handling cost for each route, and the service cost for each region, i.e.,

$$\min \sum_l \sum_{(i,j) \in \mathcal{E}_a} \hat{w}^l_{ij} \eta^l_{ij} + \sum_l \sum_k \bar{w}^l \sigma_{kl} + \sum_c \sum_{i,j \in \mathcal{B}_c} \sum_l \sum_m \tilde{w}^{m,l}_{ij} \tau^{m,l}_{ij}.$$

Figure 26. Equation. Objective function for MM2VRP.

The MM2VRP formulation involves integer variables, linear constraints, and a linear objective function. The number of variables, however, is very large, making it computationally difficult to close the duality gap in a reasonable time. For small instances, it can be solved exactly using branch-and-bound and/or cutting-plane methods provided by commercial solvers. For larger problem instances arising from servicing large and complex roadway networks, the exact solution may become intractable. However, the decision variables conceptually correspond to two subproblems, namely, the assignment problem and the routing problem, respectively, which can be naturally decoupled and solved in a hierarchical manner.

If we fix $\{z_{cl}\}$ as known, MM2VRP reduces to a single-type, multimode version of the problem, denoted as SM2VRP, which exclusively concerns the set of regions $C_l = \{c \in C : z_{cl} = 1\}$ for each type l, such that $\cup_l C_l = C$. Then, the service mode for region c can be selected from candidate modes $M_l = \{m \in M : \mu_{ml} = 1\}$. This selection is independent of the cross-regional routing decisions; hence $\{y_{cm}\}$ can be determined by minimizing the covering cost for every region individually. As such, for each l, we can construct a reduced abstract graph, where SM2VRP resembles the classical capacitated VRP except for the choices of service mode and accessing nodes that are entangled with the interregional routing decisions. If we greedily optimize these decisions, we can construct a heuristic method modified from the savings heuristics (Altinel and Öncan, 2005) to efficiently obtain a near-optimal solution.

Considering truck type l, the key steps to solve the SM2VRP are as follows. First, we compute the cost to service a single region in a route (i.e., a shuttle route) by choosing the optimal access points for each region, with the cost-minimizing mode, given by

$$\min_{i,j \in \mathcal{B}_c} (d_{oi}^l + d_{jo}^l + \min_{m \in \mathcal{M}_l} \tilde{w}_{ij}^{m,l}), \forall c,$$

Figure 27. Equation. Shuttle-routes costs.

and in so doing initialize the optimal access point(s) and service mode for each region. Suppose in the current solution, region c_1 is serviced via points $i_1, j_1 \in B_{c1}$ with mode m_1, and region c_2 is serviced via points $i_2, j_2 \in B_{c2}$ with m_2. If we consider a route $\{o, \ldots, c_1, o\}$ and another route $\{o, c_2, \ldots, o\}$, and change only access nodes that are directly affected by the merge (i.e., j_1 and i_2), we can compute the saving from the merge as

$$s_{c_1,c_2} = \min_{j \in B_{c_1}, i \in B_{c_2}} (d_{j_1o}^l + d_{oi_2}^l - d_{ji}^l + \tilde{w}_{i_1j_1}^{m_1,l} + \tilde{w}_{i_2j_2}^{m_2,l} - \min_{m \in \mathcal{M}_l} \tilde{w}_{i_1j}^{m,l} - \min_{m \in \mathcal{M}_l} \tilde{w}_{ij_2}^{m,l}), \forall c_1, c_2.$$

Figure 28. Equation. Savings of route merges.

Note that although we simply subscribe s_{c_1,c_2} with c_1, c_2, the savings are in fact path-dependent; that is, the order by which the routes are merged determines the selection of access points and hence the savings. We compensate for such a simplification by updating the savings pertinent to c_1 and c_2 using

Eq. (24) in each iteration before merging. Then, we merge the valid (i.e., not violating the capacity and route-duration constraints) pair of routes with the highest saving.

The assignment problem, in contrast, optimizes the same objective function Eq.(22) and involves only binary variables $\{z_{cl}\}$, while other variables solve the corresponding SM2VRP. A meta-heuristics, such as the simulated-annealing algorithm (Bertimas and Tsitsiklis, 1993), is suitable for selecting the optimal $\{z_{cl}\}$. Starting from a feasible solution, the algorithm randomly explores the neighborhood of the current solution, where candidates can be obtained by randomly perturbing the one-hot rows of $\{z_{cl}\}$.

The MM2VRP formulates the optimal delivery strategies under a specific demand pattern, which is regulated by the delivery headway H. As part of the tactical-phase decisions, the optimal H can be determined by solving the MM2VRP over a range of candidate values.

The integrated algorithm to solve MM2VRP is summarized in Figure 4.

Algorithm 1: MM2VRP

Initialize iteration counter, temperature
Initialize $\{z_{cl}\}_{\forall c, \forall l}$
      /* loop 1: Simulated Annealing for truck type assignment */
while *Maximum iteration not reached* **do**
  for $l \in \mathcal{L}$ **do**
    Identify $\mathcal{C}_l, \mathcal{M}_l$
    Construct abstract graphs for $\mathcal{C}_l$
    Initialize shuttle routes and compute savings
          /* loop 2: Savings heuristics for SM2VRP */
    while *Not all region processed* **do**
      Update and sort savings
      Perform valid merge with the highest saving

  Accept/reject current solution based on the objective from 2VRP
  Obtain candidate solution via random perturbation
  Update temperature

Figure 29. Chart. Algorithm for solving MM2VRP.

TRUCK-FLEET SCHEDULING

Suppose for truck type l, a set of truck routes is generated by solving the MM2VRP, each with a total duration T_k. The fleet-sizing problem finds the assignment of routes to the smallest fleet of trucks, such that the total duration of work shifts for each truck does not exceed the limit T_0. In its simplest form (Mingozzi et al., 2013), this problem can be formulated as a bin-packing problem, for which the first-fit decreasing algorithm is a very efficient, greedy approach but can yield suboptimal results.

Alternatively, this problem can be solved exactly using dynamic programming. Suppose we store the required time to complete each route in a 1-indexed array $\{T_k, k = 1, \dots\}$. Denote $F_{k'}(r)$ as the minimum number of trucks used when all routes with index $k \geq k'$ have been assigned and when the current truck has r units of time remaining in its shift. The optimal assignment must satisfy the Bellman equation:

$$F_{k'}(r) = \begin{cases} \min(F_{k'+1}(r - T_{k'}), 1 + F_{k'+1}(T_0 - T_{k'})) & \text{if } r \geq T_{k'} \\ 1 + F_{k'+1}(T_0 - T_{k'}) & \text{if } r < T_{k'} \end{cases}$$

Figure 30. Equation. Bellman equation for truck-fleet scheduling.

Here, $F_{k'+1}(r - T_{k'})$ corresponds to the situation of packing a route to the current truck, and $1 + F_{k'+1}(T_0 - T_{k'})$ corresponds to assigning a new truck. By initializing with $F_{K'+1}(r) = 0, \forall r$ and iterating backward, the minimum number of type-l trucks required is given by $\min_r F_1(r)$. The optimal assignment of routes to trucks can also be obtained by tracking the actions taken in solving Eq.(25). Subsequently, the required drone-fleet size associated with each truck can be collated as the largest fleet size required to serve every region, with the corresponding mode covered by the truck in all routes.

CHAPTER 4: NUMERICAL RESULTS AND CASE STUDY

In this section, we apply the proposed design framework to a series of numerical examples. The design framework is implemented in Python, with FEniCS (Logg et al., 2012) used for the finite-element functionalities, Tensorflow (Abadi et al., 2016) for the machine learning functionalities, and Gurobi (Gurobi, 2021) as the mixed-integer program solver. All numerical cases are run on a personal computer with a 2.3-GHz CPU and 16-GB RAM.

The parameters of the congestion function used in MTD mode, which facilitates a density-based function, are the same as those used by She and Ouyang (2022), based on which the parameters used in DD and STD modes, where a flux-based function is used, are determined such that key quantities (e.g., maximum flux capacity and stagnation density) are in accordance. For the drones' operating cost, we take c_d = \$0.5/drone-hr and w_{df} = \$1/drone (Sudbury and Hutchinson, 2016).

We consider two types of trucks. Type-1 truck is the conventional delivery truck currently used by the industry and can be used only for the truck-only delivery mode, for which we assume take trucking cost c_t^1 = \$3/mi (Williams and Murray, 2020). Type-2 truck is equipped with drone-launching and -charging functionalities and is compatible with STD and MTD modes. It can also be used for conventional truck-only delivery if desired. There is not yet any credible estimation of the commercial price for such enhancement of compatibility. We first preliminarily assume c_t^2 = c_t^1 = \$3/mi and will examine its impact on operational decisions in later analysis. Meanwhile, we assume both truck types incur dispatching cost $\bar{c}^1$ = $\bar{c}^2$ = \$50 per dispatch and have the same capacity of 1,000 parcels. Either type of truck is operated by a deliverer paid a salary of \$30/hr. The waiting cost is assumed w_c = \$0.001/parcel-hr (Murray and Glidewell, 2019). We use a safe maximum speed for drones of 50 mph and a cruising speed for trucks of 30 mph.

We first construct the cost envelope, which provides a convenient reference for selecting the delivery mode in solving the SM2VRP. Consider a city where streets form perfect square grids of spacing 0.1 mi; a single circular demand region of area A square miles, the same as those presented in Figure 1; anda depot located S mi away from the center of the region, from which the logistic carrier dispatches vehicles to conduct delivery. We assume that the logistics carrier conducts daily delivery, during which period the demand region generates a regulated demand rate ρ_0. For a range of combinations of ρ_0 and A, where $\rho_0 \in \{10, 50, 100, 200, 400, 1,000, 10,000, 50,000, 100,000\}$ parcels per sq mi per day and $A \in \{0.25, 0.5, 1, 2, 4\}$ mi, we estimate the expected delivery cost per parcel using each mode. For the truck-only mode, which involves truck routing dependent on the realized demand, 20 sets of demand points are randomly drawn to determine the truck routes; and the average delivery cost is used. Taking S = 10 and slicing at A = 1, the delivery cost of each mode with respect to demand density is shown in Figure 5. The minimum of the four curves provides a cost envelope that indicates the optimal choice of delivery mode serving the region. As the most labor-intensive mode, conventional truck-only delivery incurs a service time proportional to the demand rate.

Not surprisingly, the truck-only delivery mode is the least favorable mode under all demand levels due to the long service time, particularly when the labor cost is relatively expensive. Under low

demand density, the MTD mode demonstrates a similar trend to that of the truck-only mode, mainly due to the dominating trucking cost along a covering path. To the contrary, the STD mode incurs less truck-traveled distance and hence saves on the trucking cost. The DD mode does not involve trucking, hence incurs a much lower cost per delivery when the demand level is low. As the demand-density level rises, the service time of the truck-only delivery mode quickly violates the 24-hr-wall time constraints as the demand rate exceeds 400. The delivery cost for drone-based modes appears insensitive until the demand rate ramps up beyond 50,000, where aerial congestion starts significantly to impede delivery efficiency. The key merit of the MTD mode, as distinct from the DD and STD modes, is in the processing rate of demand; or equivalently, the number of drones simultaneously operating in the system. As a result, the delivery cost increases with a lower curvature, mainly due to the meliorated aerial congestion and the smaller fleet size required.
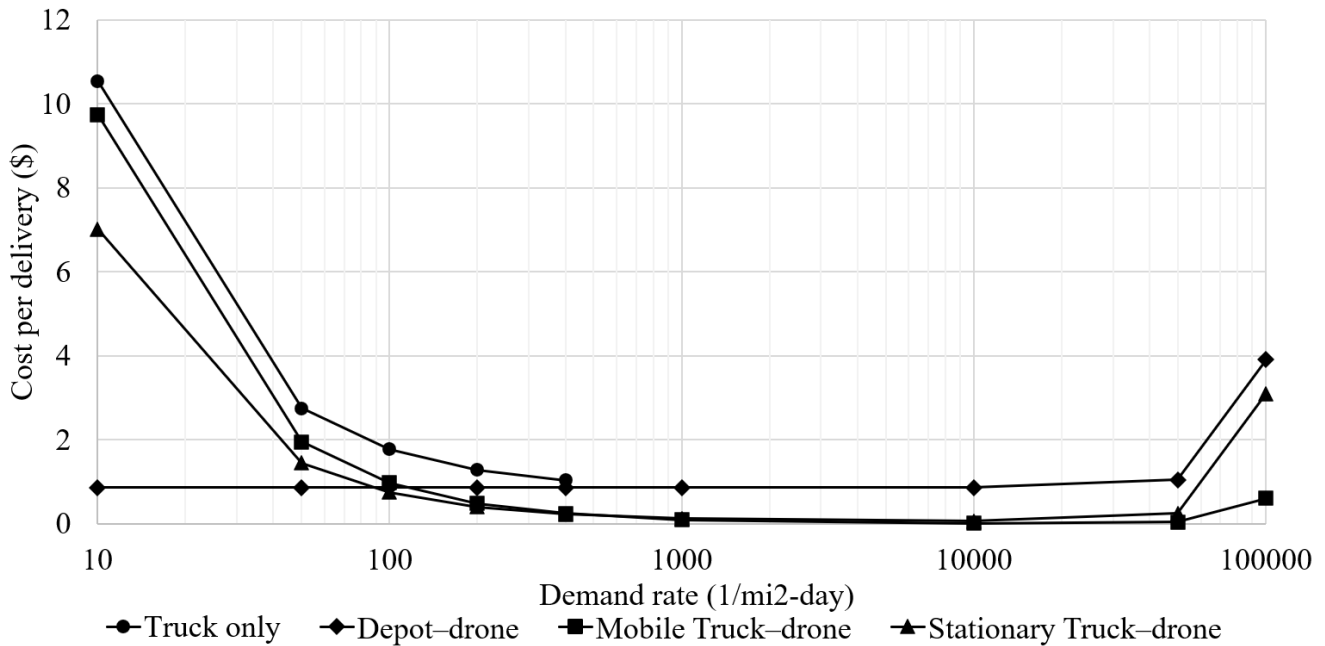
Figure 31. Graph. Delivery-cost comparison vs. demand level.

Similarly, we slice at $\rho_0 = 400$ and plot the delivery cost per parcel for the four modes with respect to the area of the demand region in Figure 6. The conventional delivery mode is again the least favored among the values examined. The average delivery cost for the DD mode gradually increases with area size, due to the increasing length for serving distant customers and the ramping congestion. Overall, the size of the demand region demonstrated a similar impact on the average delivery cost.
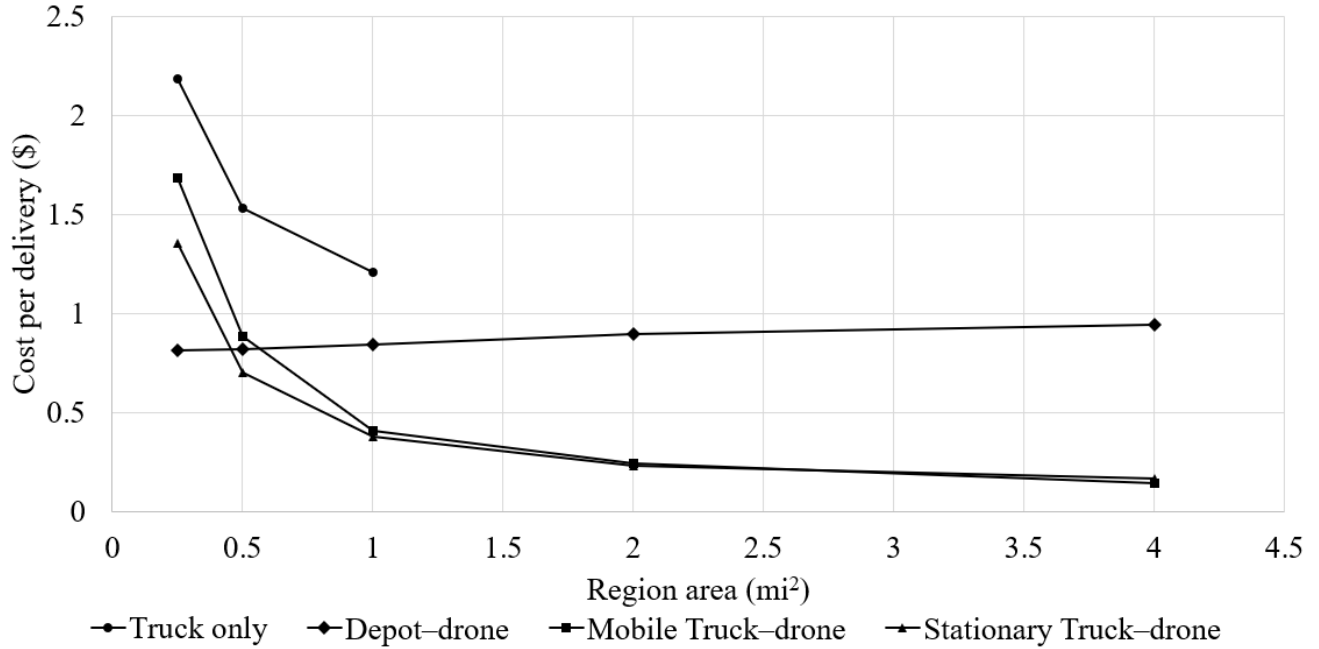
**Figure 32. Graph. Delivery-cost comparison vs. delivery-region size.**

We then illustrate the applicability of the design framework to real roadway networks, for which we take Rantoul, Illinois, USA, as an example. Six residential clusters are identified from the demographic survey; each generates a delivery-demand density of 200 per sq mi. A warehouse located at the southwest corner serves as the depot. Such a low demand level over a relatively small network promotes DD as the most favorable delivery mode. For illustrative purposes, we consider serving all regions with the MTD mode. Figure 7a shows a demand instance, and Figure 7b and Figure 7c show the corresponding routing strategy yielded by both solving the single-type, single-model 2VRP exactly using Gurobi and using the proposed heuristics, respectively. The Gurobi solver on average yielded an average delivery cost of $1.12 per parcel, and the proposed heuristics yielded $1.63 per parcel. Such a routing strategy can be fulfilled with just one truck at 42 drones. Such a gap is mainly due to the underperformance of the swath-based covering path algorithm on non-regular networks. In this example, the exact solution can be computed within 5 min, while the heuristics yield the result in 20 sec.

As the network grows, exactly solving the MM2VRP formulation becomes computationally prohibitive. Consider the urban area of Chicago, Illinois, which encloses a square area of 10 miles on the side. Several demand regions are identified, as presented in Figure 8a. In each of these regions, we postulate a demand distribution given by

$$\bar{\rho}_0(\mathbf{x}) = \max(0, 500 - 100\lfloor |\mathbf{x} - \mathbf{x}(n_c)|_\infty / 0.5 \rfloor), \forall c.$$

**Figure 33. Equation. Demand pattern.**

Such a function generates a demand distribution peaked at the square around the center and gradually decreases by 0.5-mi-wide stages at locations moving away from the center, as illustrated in Figure 9. With the insights brought by the cost envelopes, we can safely regard the truck-only delivery mode as inferior and consider only the other three modes. The result of route planning is shown in Figure 8b. In this network, even the precomputation of covering costs cannot be completed in 6 hr; and for the given covering costs, the MM2VRP cannot be solved exactly in another 6-hr-wall time. In contrast, the heuristics-based design procedure completes in less than 30 min. In this instance, the demand is serviced at an average cost of $1.94 per parcel with 9 trucks and 737 drones.
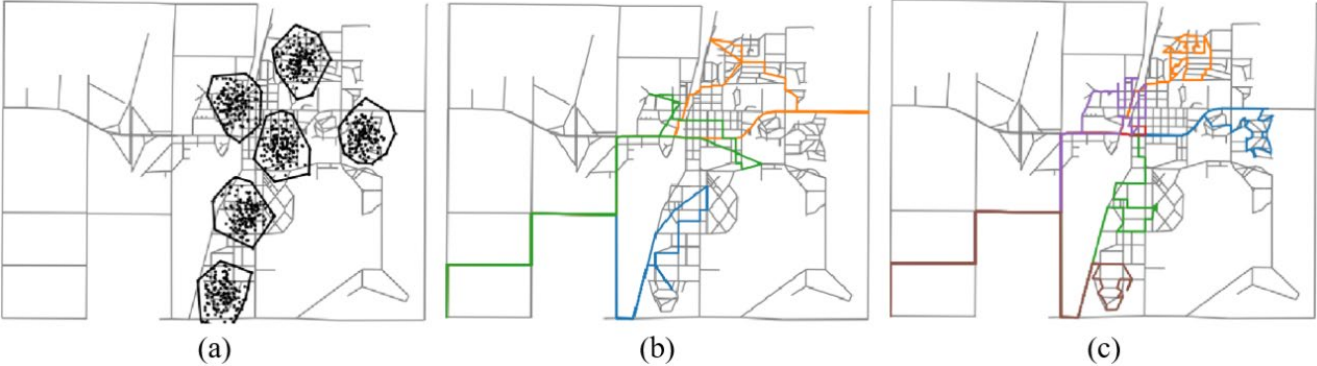
Figure 34. Diagram. Rantoul, Illinois, example: (a) demand regions, (b) routes yielded by Gurobi, (c) routes yielded by heuristics.

Figure 35. Diagram. Chicago, Illinois, example: (a) demand regions, (b) delivery routes.
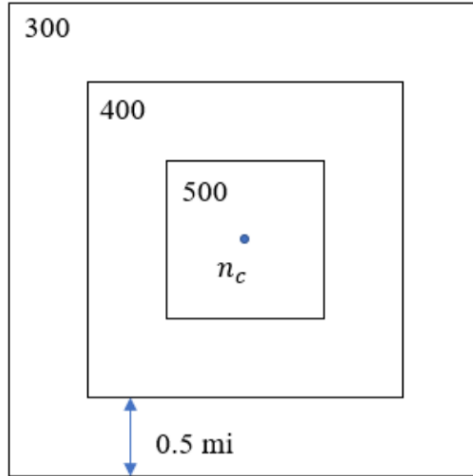
Figure 36. Diagram. A hypothetical demand distribution.

We now turn our attention back to the city with perfect grid streets and conduct further analysis to draw operational insights. Suppose the city spans a square 10 miles on the side and generates demand according to Eq.(9) from its center. The logistics carrier operates the delivery from a depot located at the southwest corner of the city. Figure 9b plots performance metrics of the results by solving the MM2VRP with respect to the delivery headway, which regulates the demand level. The delivery cost per parcel is plotted as the curve and demand percentages served by each mode as clustered columns. It can be observed that, in accordance with Figure 5, the DD mode is dominant under low demand levels. As demand accumulates, the DD mode and even the STD mode become warranted, mainly due to the trucking cost being diluted over the demands served. Overall, the delivery cost reduces as the delivery headway elongates; and for the illustrated instance, the longest allowed headway of 4 days is optimal.

Among the said parameters, the logistics carrier may be specifically interested in the trucking cost and capacity of the type-2 truck, which largely influence the economical efficiency of the hybrid delivery schemes as an alternative to conventional delivery. We determine the optimal delivery strategies under a range of trucking cost $c_t^2 \in \{0, 1, 2, 3, 5, 10\}$ dollars and plot the corresponding performance metrics in Figure 10. Not surprisingly, as the trucking cost increases, the delivery cost also increases as the trucking component becomes more expensive. Meanwhile, the percentage of DD mode increases, as other modes involving trucking become less profitable. When the trucking cost reaches $10 per mi, the DD mode dominates for the given network. We conduct a similar analysis with respect to $Q^2 \in \{500, 1{,}000, 1{,}500, 2{,}000\}$ and plot in Figure 11. As truck capacity increases, trucks can cover more partitioned areas, potentially allowing more efficient routes. Consequently, more demands are better served with hybrid truck–drone delivery (i.e., STD and MTD); and the average delivery cost is reduced.
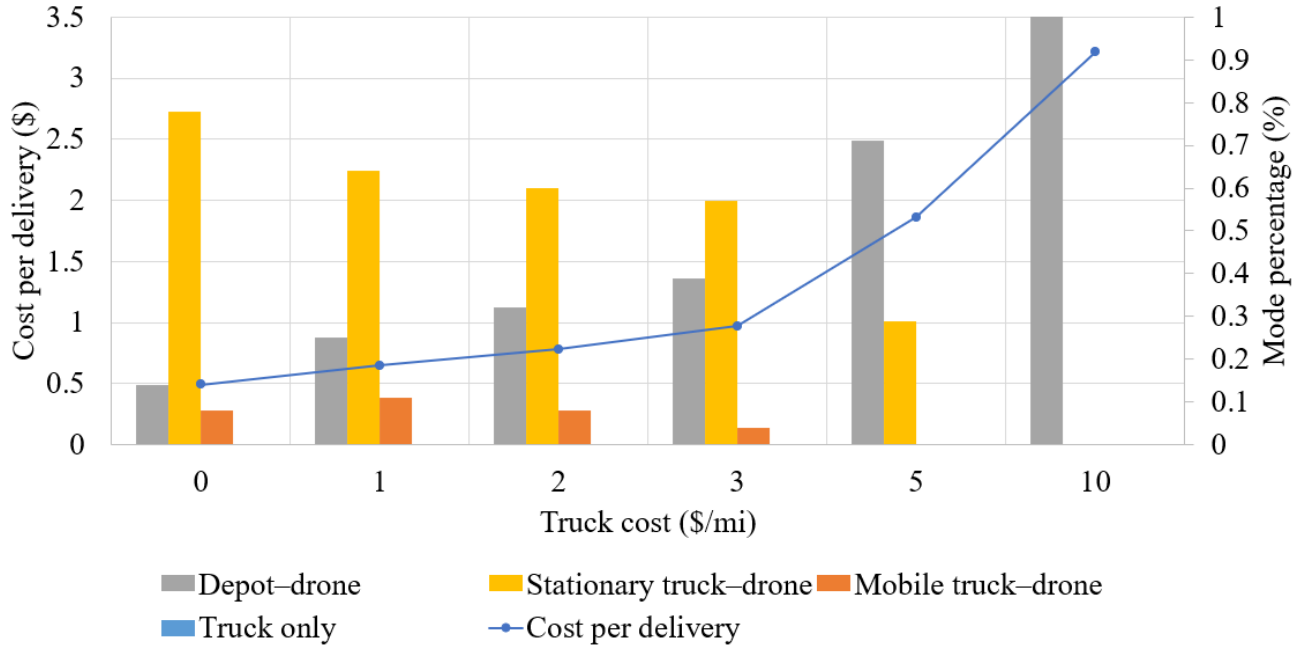
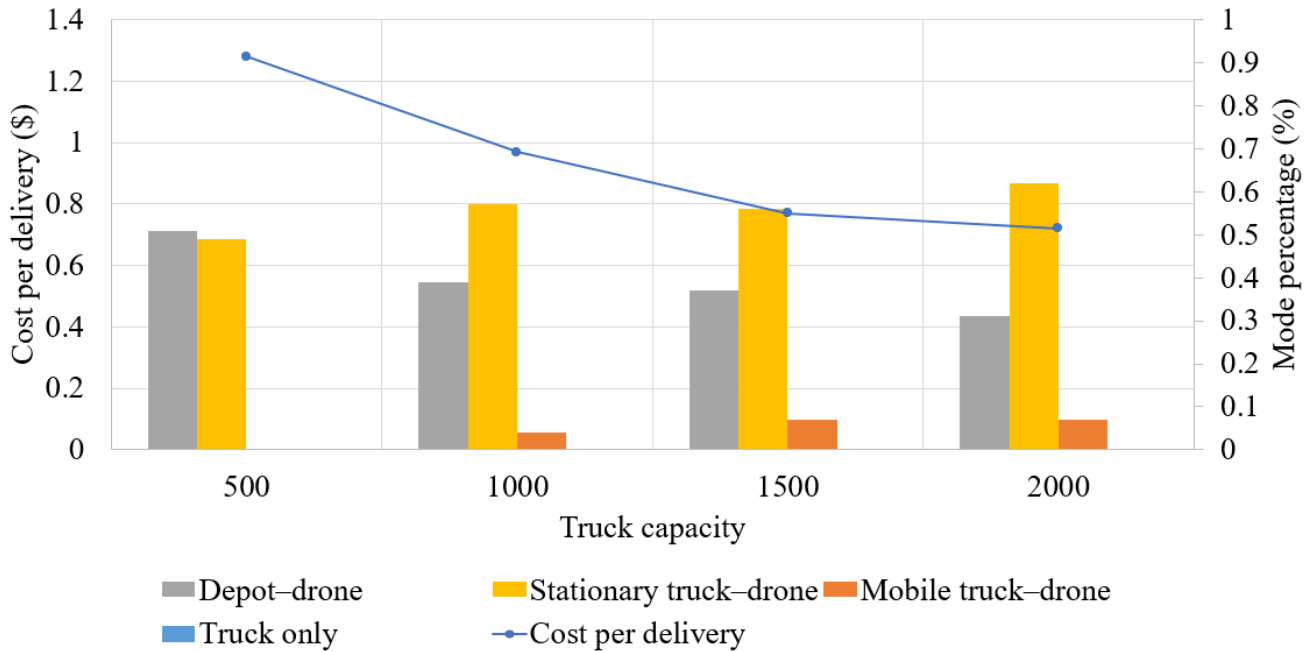**Figure 37. Graph. Cost per delivery and mode percentage with respect to delivery headway.**

Figure 38. Graph. Cost per delivery and mode percentage with respect to the cargo capacity of trucks,

CHAPTER 5: CONCLUSION AND FUTURE RESEARCH

This paper presents an integrated design framework for a drone-based delivery system, combining drones and trucks to optimize last-mile deliveries. The framework incorporates multiple delivery modes and vehicle types, allowing for flexible and efficient delivery operations. By using a partition-routing approach, the delivery domain is divided into regions, each serviced by a specific mode and type of vehicle. The framework considers four delivery modes: depot–drone, stationary truck–drone, mobile truck–drone, and truck-only delivery. The collective routing decisions of both trucks and drones are modeled in a variant of the multi-type, multimode vehicle-routing problem as a mixed-integer program. An efficient heuristic algorithm is proposed to solve each component in the integrated design framework. To support decision-making, a cost envelope is constructed to compare the performance of these modes. The applicability of the model is demonstrated on real roadway networks. Numerical analyses are conducted on a grid network to draw insights into the impact of key operational parameters.

The research presented in this paper can be extended in several directions. First, the heuristic algorithm used for solving the covering-path problem could be enhanced to provide more efficient solutions for general and complex graphs. This process could involve adaptive modifications to improve computational efficiency without sacrificing performance. Second, the cost envelope, which largely governs the selection of delivery mode, is a numerical result of hypothetical parameters defining local travel costs, particularly the drones' congestion function. Further calibration, either with simulation or experiments, is needed to enhance the strength of reference of the cost envelope. Third, in evaluating the local delivery cost with the mobile truck–drone scheme, a surrogate model was constructed by solving the PDEs using PINN under various configurations. A recent thread of research explores the possibility of using PINN to evaluate directly the gradient of operation cost with respect to design parameters, such as truck speed or demand rate, so as to integrate the PDE solution into a gradient-based design model that optimizes operational decisions. Finally, in the current design framework, the vehicle-fleet sizes for trucks and drones are determined so as to support the operational strategies that minimize the average delivery cost. The fleet sizes can also be integrated into the design framework as decision variables that significantly impact the decision-making of all subproblems.

REFERENCES

Abadi, Martín, (2016). "TensorFlow: a system for Large-Scale machine learning." In *12th USENIX symposium on operating systems design and implementation (OSDI 16)*.

Altınel, İ. K., and Temel Öncan (2005). "A new enhancement of the Clarke and Wright savings heuristic for the capacitated vehicle routing problem." *Journal of the Operational Research Society, 56:* 954–961.

Bertsimas, Dimitris, and John Tsitsiklis (1993). "Simulated annealing." *Statistical Science, 8*(1): 10–15.

Carlsson, John Gunnar, and Siyuan Song (2018). "Coordinated logistics with a truck and a drone." *Management Science, 64*(9): 4052–4069.

Chauhan, Darshan Rajesh, Avinash Unnikrishnan, and Stephen D. Boyles (2022). "Maximum Profit Facility Location and Dynamic Resource Allocation for Instant Delivery Logistics." *Transportation Research Record: Journal of the Transportation Research Board, 2676*(7): 697–710.

Chiang, Wen-Chyuan, Yuyu Li, Jennifer Shang, and Timothy L. Urban. (2019). "Impact of drone delivery on sustainability and cost: Realizing the UAV potential through vehicle routing optimization." *Applied Energy, 242:* 1164–1175.

Choset, Howie (2000). "Coverage of known spaces: The boustrophedon cellular decomposition." *Autonomous Robots, 9:* 247–253.

Christofides, Nicos, Aristide Mingozzi, and Paolo Toth (1981). "Exact algorithms for the vehicle routing problem, based on spanning tree and shortest path relaxations." *Mathematical programming*, *20:* 255–282.

Corberán, Angel, Rafael Martí, and Antonio Romero (2000). "Heuristics for the mixed rural postman problem" *Computers & Operations Research*, *27*(2): 183–203.

Daganzo, Carlos F. (1984). "The length of tours in zones of different shapes." *Transportation Research Part B: Methodological*, *18*(2): 135–145.

Dorling, Kevin, Jordan Heinrichs, Geoffrey G. Messier, and Sebastian Magierowski. (2016). "Vehicle routing problems for drone delivery" *IEEE Transactions on Systems, Man, and Cybernetics: Systems, 47*(1): 70–85.

Du, Qiang, Maria Emelianenko, and Lili Ju (2006). "Convergence of the Lloyd algorithm for computing centroidal Voronoi tessellations." *SIAM Journal on Numerical Analysi, 44*(1): 102–119.

Fahim, Ahmed (2018). "Homogeneous densities clustering algorithm." *IJ Information Technology and Computer Science, 10*(10): 1–10.

Frachtenberg, Eitan (2019). "Practical drone delivery." *Computer*, *52*(12): 53–57.

Francis, Peter M., Karen R. Smilowitz, and Michal Tzur (2008). "The period vehicle routing problem and its extensions." *The vehicle routing problem: latest advances and new challenges*, Springer, 73–102.

Gurobi Optimization LLC (2021). *Gurobi optimizer reference manual*.

Helsgaun, Keld (2000). "An effective implementation of the Lin–Kernighan traveling salesman heuristic." *European Journal of Operational Research*, *126*(1): 106–130.

Jokisch, Oliver, and Dominik Fischer (2019). "Drone sounds and environmental signals–a first review." In *Proceedings of the ESSV Conference (Studientexte zur Sprachkommunikation), 93*.

Kim, Miae, and Eric T. Matson (2017). "A cost-optimization model in multi-agent system routing for drone delivery." In *Highlights of Practical Applications of Cyber-Physical Multi-Agent Systems: International Workshops of PAAMS 2017, Porto, Portugal, June 21-23, 2017, Proceedings 15*. Springer International Publishing.

Laporte, Gilbert (2009). "Fifty years of vehicle routing." *Transportation Science*, *43*(4): 408–416.

Liang, Yi-Jing, and Zhi-Xing Luo (2022). "A survey of truck–drone routing problem: Literature review and research prospects." *Journal of the Operations Research Society of China, 10*(2): 343–377.

Logg, Anders, Kent-Andre Mardal, and Garth Wells, eds. (2012). *Automated solution of differential equations by the finite element method: The FEniCS book*, *84.* Springer Science & Business Media, 2012.

Mingozzi, Aristide, Roberto Roberti, and Paolo Toth (2013). "An exact algorithm for the multitrip vehicle routing problem." *INFORMS Journal on Computing,25*(2): 193–207.

Murray, Chase C., and Amanda G. Chu (2015). "The flying sidekick traveling salesman problem: Optimization of drone-assisted parcel delivery." *Transportation Research Part C: Emerging Technologies*, *54:* 86–109.

Murray, Chase C., and Ritwik Raj (2020). "The multiple flying sidekicks traveling salesman problem: Parcel delivery with multiple drones." *Transportation Research Part C: Emerging Technologies*, *110:* 368–398.

Murray, Dan, and Seth Glidewell (2019). An analysis of the operational costs of trucking: 2019 update. Technical Report, American Transportation Research Institute.

Nobert, Yves, and Jean-Claude Picard (1996). "An optimal algorithm for the mixed Chinese postman problem." *Networks: An International Journal*, *27*(2): 95–108.

Pachayappan, Murugaiyan, and Vijayakumar Sudhakar (2021). 'A solution to drone routing problems using docking stations for pickup and delivery services." *Transportation Research Record: Journal of the Transportation Research Board, 2675*(12): 1056–1074.

Palmer, Annie (2020, August 31) . Amazon wins FAA approval for prime air drone delivery fleet. *CNBC*. https://www.cnbc.com/2020/08/31/amazon-prime-now-drone-delivery-fleet-gets-faa-approval.html

Park, Junhyuk, and Byung-In Kim (2010). "The school bus routing problem: A review." *European Journal of Operational Research*, *202*(2): 311–319.

Perlow, B. (2016, December 15). Amazon completes 1st drone delivery. *ABC News*. https://abcnews.go.com/US/amazon-completes-drone-delivery/story

Schubert, Erich, Jörg Sander, Martin Ester, Hans Peter Kriegel, and Xiaowei Xu. (2017). "DBSCAN revisited, revisited: why and how you should (still) use DBSCAN." *ACM Transactions on Database*

Systems (TODS), *42*(3): 1–21.

Shavarani, Seyed Mahdi, Sam Mosallaeipour, Mahmoud Golabi, and Gökhan İzbirak. (2019). "A congested capacitated multi-level fuzzy facility location problem: An efficient drone delivery system." *Computers & Operations Research, 108:* 57–68.

She, Ruifeng, and Yanfeng Ouyang (2022). "Hybrid Truck-Drone Delivery Under Aerial Traffic Congestion." Available at SSRN 4189367.

She, Ruifeng, and Yanfeng Ouyang (2021). "Efficiency of UAV-based last-mile delivery under congestion in low-altitude air." *Transportation Research Part C: Emerging Technologie, 122:* 102878.

Sudbury, Adrienne Welch, and E. Bruce Hutchinson (2016). "A cost analysis of Amazon Prime air (drone delivery)." *Journal for Economic Educators*, *16*(1): 1–12.

Wang, Xiaoqun, and Fred J. Hickernell (2000). "Randomized halton sequences." *Mathematical and Computer Modelling*, *32*(7/8): 887–899.

Wang, Zheng, and Jiuh-Biing Sheu (2019). "Vehicle routing problem with drones." *Transportation Research Part B: Methodological*, *122:* 350–364.

Wardrop, John Glen (1952). "Road paper: Some theoretical aspects of road traffic research." In *Proceedings of the Institution of Civil Engineers*, *1*(3): 325–362.

Williams, Nathan, and Dan Murray (2000). An analysis of the operational costs of trucking: 2020 update., Technical Report, American Transportation Research Institute.

Zeng, Liwei, Sunil Chopra, and Karen Smilowitz (2019). "The covering path problem on a grid." *Transportation Science*, *53*(6): 1656–1672.

Zoldi, Dawn (2021). "Drone law and policy." *Scitech Lawyer, 17*(3):12–17, 2021.